

## Mars at Low Obliquity: Perennial CO<sub>2</sub> Caps, Atmospheric Collapse, and Subsurface Warming.

Stephen E. Wood<sup>1</sup>, Stephen D. Griffiths<sup>2</sup>, and Jonathan N. Bapst<sup>1</sup>, Dept. of Earth and Space Sciences, University of Washington, Box 351310, Seattle, WA, 98195-1310, sewood@ess.washington.edu, <sup>2</sup>Dept. of Applied Mathematics, University of Leeds, Leeds, LS2 9JT, UK.

**Introduction:** At low obliquity the polar regions of Mars receive less annual insolation and can reach a point where the total CO<sub>2</sub> sublimation at the pole becomes less than the total condensation – forming a perennial CO<sub>2</sub> ice polar cap. Below this critical obliquity the mass of the CO<sub>2</sub> polar cap(s) increases at the expense of the atmosphere, potentially leading to atmospheric “collapse”. Recent radar evidence for a massive buried deposit of CO<sub>2</sub> ice within the south polar layered deposits presented by Phillips *et al.* (2011) [1] has bolstered the case for this scenario. An important consequence of this pressure drop is that it can cause a significant decrease in the thermal conductivity of uncemented porous regolith materials [2]. This effect, which has not been considered previously in studies of Mars’ climate, can lead to increased subsurface temperatures as the planetary heat flow becomes trapped below a more insulating upper layer [3]. The degree of subsurface warming depends strongly on the minimum atmospheric pressure reached, as well as the assumed heat flow, but has the potential to produce episodic liquid water by melting deep ground ice or dewatering of hydrated minerals. Even in the absence of melting, this warming could have significant geomorphic effects by increasing flow rates of buried ice such as lobate debris aprons. At the very least, it would cause the loss or vertical redistribution of as much as 5000 kg/m<sup>2</sup> of ground ice (or ~25 m of 20%-porosity-filling ice) during each low obliquity period.

While the precise magnitude of atmospheric collapse at low obliquity is uncertain, the fact that a significant decrease in atmospheric pressure can occur is a robust conclusion for a wide range of realistic values of CO<sub>2</sub> frost albedo ( $A_f$ ) and emissivity ( $\epsilon_f$ ) (**Fig. 1**). Values of  $A_f$  and  $\epsilon_f$  obtained as best-fits in models of the seasonal pressure cycle may not be representative of the entire seasonal CO<sub>2</sub> polar cap because the atmospheric mass is most strongly affected by the lower latitude portions (50°–70°) where they have the greatest surface area [4], and where they are more likely to be affected by dust storms. Observational studies have shown that the central portions of the seasonal polar caps can be much brighter than the outlying portions, with springtime  $A_f$  values as high as 0.83 and  $\epsilon_f$  close to unity [5] (see Fig. 1).

**Model:** We have performed seasonally-resolved calculations of the evolution of Mars’ atmospheric

pressure over the past 1 Myr using a model [3] that includes subsurface heat conduction and the latest calculations of Mars’ orbital and axial variations [8]. The zonally-symmetric model calculates the amount of surface CO<sub>2</sub> condensation or sublimation 12 times per year at 23 latitudes (clustered near the poles) based on a surface energy balance using daily average insolation rates. Subsurface heat conduction is computed using a semi-implicit numerical scheme (~2<sup>nd</sup> order accuracy) using 40 vertical gridpoints divided into 2 layers with differing thermal properties (Chebyshev spacing in each layer with flux matching at interface). Zonally-

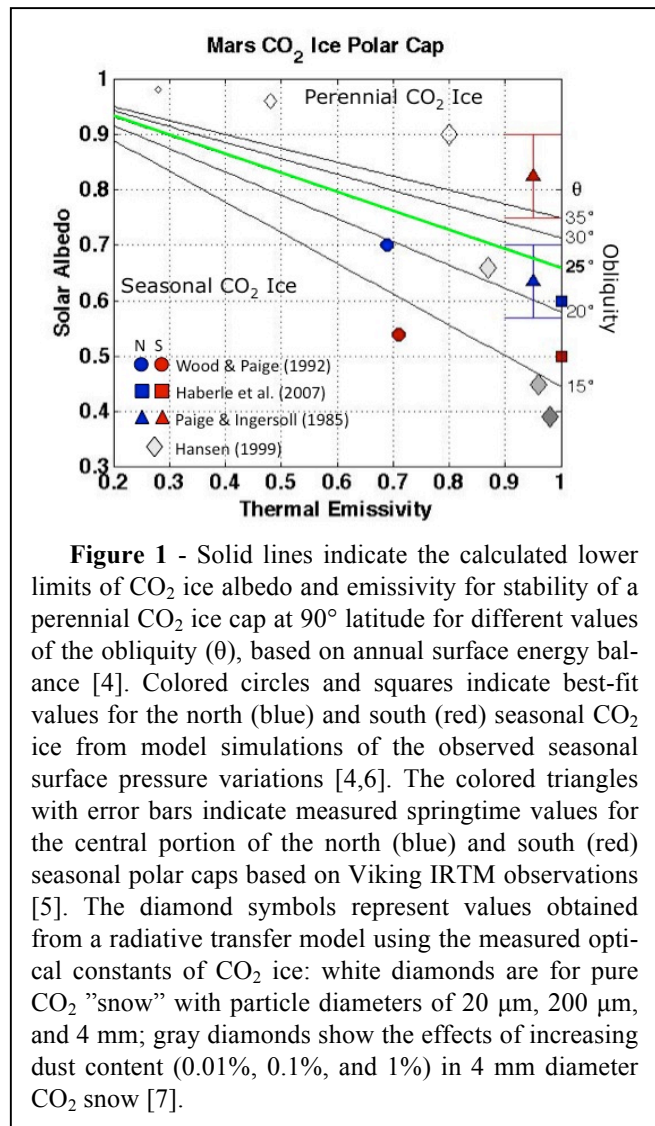


**Figure 1** - Solid lines indicate the calculated lower limits of CO<sub>2</sub> ice albedo and emissivity for stability of a perennial CO<sub>2</sub> ice cap at 90° latitude for different values of the obliquity ( $\theta$ ), based on annual surface energy balance [4]. Colored circles and squares indicate best-fit values for the north (blue) and south (red) seasonal CO<sub>2</sub> ice from model simulations of the observed seasonal surface pressure variations [4,6]. The colored triangles with error bars indicate measured springtime values for the central portion of the north (blue) and south (red) seasonal polar caps based on Viking IRTM observations [5]. The diamond symbols represent values obtained from a radiative transfer model using the measured optical constants of CO<sub>2</sub> ice: white diamonds are for pure CO<sub>2</sub> “snow” with particle diameters of 20  $\mu$ m, 200  $\mu$ m, and 4 mm; gray diamonds show the effects of increasing dust content (0.01%, 0.1%, and 1%) in 4 mm diameter CO<sub>2</sub> snow [7].

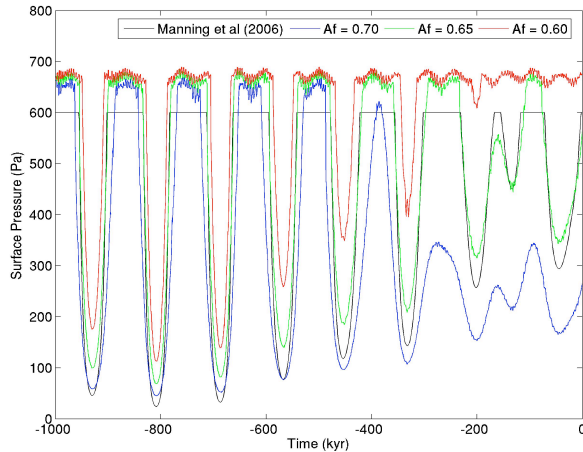


**Figure 2** – Model-calculated variations in global mean surface pressure for the past  $10^6$  years, with our results (colored lines) compared to those of Manning et al (2006). Our model results shown here were obtained using a CO<sub>2</sub> frost emissivity of 1.0 and three different values of CO<sub>2</sub> frost albedo, held constant throughout each simulation. Our simulations assumed a slightly greater mass of CO<sub>2</sub> in the cap-atmosphere system making the maximum pressures higher.

averaged Viking IRTM soil albedo and thermal inertia values were used for the upper layer at each latitude, with zonally-averaged MOLA topography to calculate local atmospheric surface pressure and CO<sub>2</sub> frost temperature [3]. We found that for values of  $A_f = 0.60$ , 0.65, and 0.70 (with  $\epsilon_f = 1.0$  in all cases), the minimum pressures reached were 113 Pa, 69 Pa, and 45 Pa, respectively (**Fig. 2**). In our model, the lowest possible pressure is 29 Pa, due to the presence of 7.9 kg/m<sup>2</sup> of non-condensable gases.

The first long-term climate model that included a seasonally-resolved model of polar energy balance [9] used values of  $A_f = 0.67$  and  $\epsilon_f = 0.55$  that precluded the formation of perennial CO<sub>2</sub> ice caps unless the obliquity was less than 13°, and therefore predicted no atmospheric collapse during the past 10 Myr. The first long-term climate model to include the latest calculations of Mars’ orbital and axial variations [8] predicted a minimum pressure of 30 Pa in the past 1 Myr, using  $A_f=0.70$  and  $\epsilon_f=1.0$ , but did not include the effects of subsurface heat conduction [10]. The Manning et al. 2006 model [10] did include a parameterized treatment of atmospheric heat transport, but this is less significant during periods of atmospheric “collapse”. The comparison in Fig. 2 shows that using the same values of  $A_f$  and  $\epsilon_f$  our model predicts similar minimum pressures prior to 300 kya, but the predicted global mean pressure on present-day Mars is much lower than observed. This is due to the predicted stability of a peren-

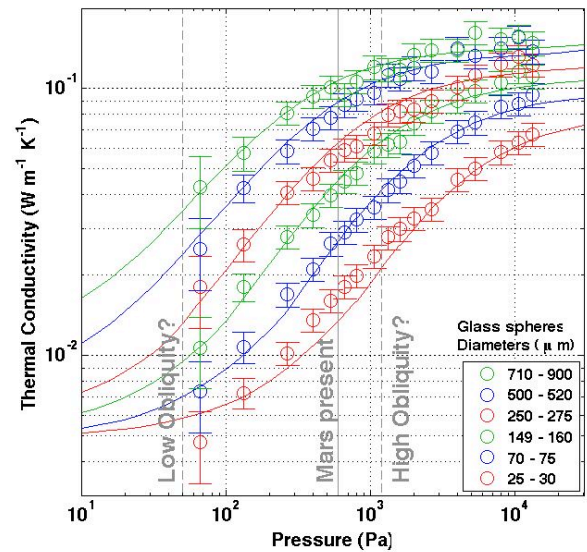


**Figure 3** – Laboratory measurements (symbols) of the thermal conductivity of silica glass beads in CO<sub>2</sub> gas as a function of gas pressure and particle size [Presley & Christensen (1997)] along with model-calculated values (lines) using the analytic model of Wood [2011]. These show the expected decrease in conductivity at lower pressures as the mean free path of gas molecules becomes limited by the dimensions of the pore space. Vertical gray lines indicate the mean atmospheric pressure on Mars at present (solid gray) and its potential range due to obliquity variations (dashed gray).

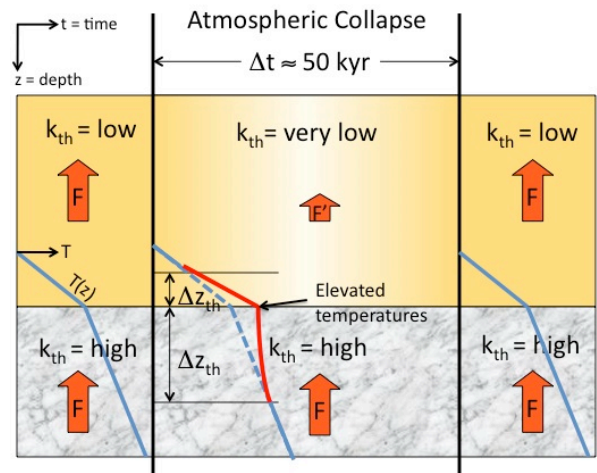


**Figure 4** – Schematic illustration of the possible effects of atmospheric collapse on subsurface thermal conductivity, geothermal heat flux, and the temperature profile. Time progresses from left to right and the vertical dimension represents depth with a porous “loose” regolith surface layer overlying a more consolidated layer (such as sandstone or ice-cemented soil) whose conductivity is less sensitive to pore gas density. The blue lines indicate the temperature profile before and after a low obliquity period when the geothermal heat flux is approx. equal in both layers and  $dT/dz$  is proportional to  $k_{th}$ .

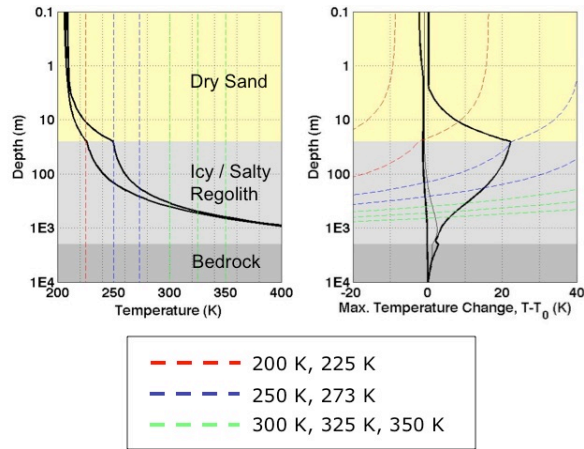


**Figure 5** – *Left panel*: Minimum and maximum subsurface temperatures (solid black lines) reached during a 200 kyr period spanning the obliquity minimum at  $\sim 800$  kya (see Fig. 2). Dashed lines indicate isotherms at specific temperatures for reference. *Right panel*: Temperature differences with respect to the temperature profile at the beginning of the modeled 200 kyr period for the max. and min. temperatures shown in the left panel (thick black lines) as well as for the temperature profile at the end of the 200 kyr period (thin black line).

nial CO<sub>2</sub> ice polar cap at the north pole (and not in the south) for this high albedo case ( $A_f=0.70$ ).

**Perennial CO<sub>2</sub> ice** is actually observed today at the south pole (and not in the north), although it appears to be just a few meters thick and it is not known whether it is currently experiencing net sublimation or accumulation on multiyear timescales [11]. We note, however, that the north would usually be the preferred pole for perennial CO<sub>2</sub> ice formation if CO<sub>2</sub> ice radiative properties are the same in both hemispheres. This is because the nearly pure (95%) CO<sub>2</sub> atmosphere of Mars maintains the temperature of surface CO<sub>2</sub> ice at the solid-vapor equilibrium temperature and the lower elevation of the north polar region results in higher CO<sub>2</sub> ice temperatures (due to higher atmospheric pressure) which enables greater radiative cooling during polar night and this is the primary sink for the latent heat of CO<sub>2</sub> condensation. Spacecraft observations show that the springtime albedo of seasonal CO<sub>2</sub> frost is quite variable in time and space, with no clear hemispheric dependence. But observations restricted to the residual cap areas showed that  $A_f$  was significantly higher in the south than in the north (Fig. 1), and that in both hemispheres there was a strong correlation with insolation (see Fig. 7) [5].

**Insolation-dependent CO<sub>2</sub> frost albedo**: Guo et al. (2010) [12] performed simulations of the seasonal CO<sub>2</sub> cycle with a Mars GCM using an insolation dependent CO<sub>2</sub> frost albedo based on Viking IRTM ob-

servations (see Fig. 7). They found that including this effect produced a stable perennial CO<sub>2</sub> south polar ice cap near the south pole for the present orbital configuration, similar to what is actually observed on Mars, due to the current proximity of southern summer season to perihelion resulting in 45% greater peak insolation at the south pole and corresponding 20% higher  $A_f$ . The albedo effect then outweighs the elevation effect described above. Interestingly, as Guo et al (2010) point out, an insolation-dependent  $A_f$  can also lead to stable perennial CO<sub>2</sub> caps at high obliquity as well. This effect is also seen in our model simulations (e.g., Fig. 8).

**Atmospheric Inflation?**: The total mass of buried CO<sub>2</sub> ice recently discovered near the south pole is estimated to be  $\sim 80\%$  of the present global atmospheric mass [1]. If this reservoir was released into the atmos-

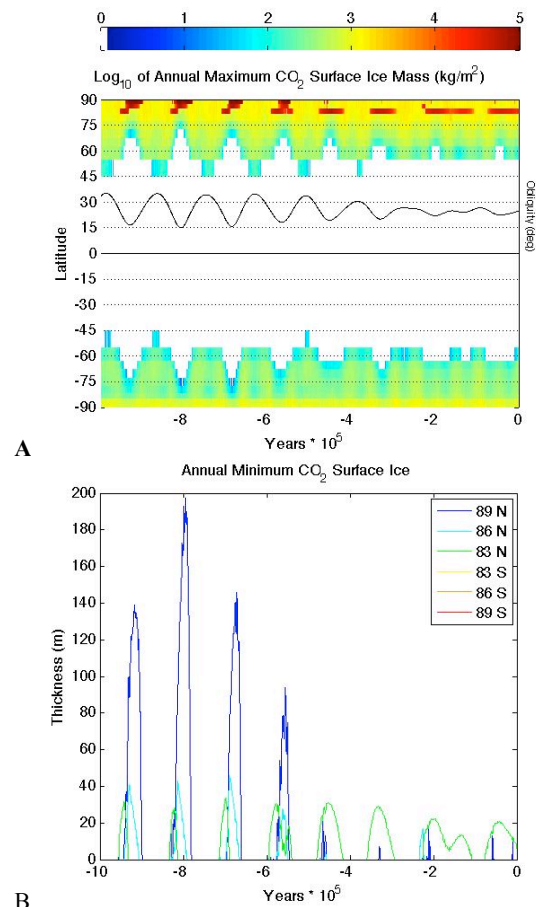


**Figure 6** – Results for model with  $A_f = 0.65$  and  $e_f = 1.0$  for CO<sub>2</sub> surface ice (corresponding pressure variations shown in Fig. 2 as green line). (A) Colors indicated the annual maximum mass (per unit area) of CO<sub>2</sub> ice as a function of latitude and time for the past 1 Myr. The black curvy line indicates obliquity for reference. Areas colored red generally correspond with locations of perennial CO<sub>2</sub> ice. (B) Annual min. thickness of CO<sub>2</sub> ice predicted at several polar latitudes, calculated assuming a solid ice density of  $1600 \text{ kg/m}^3$ .

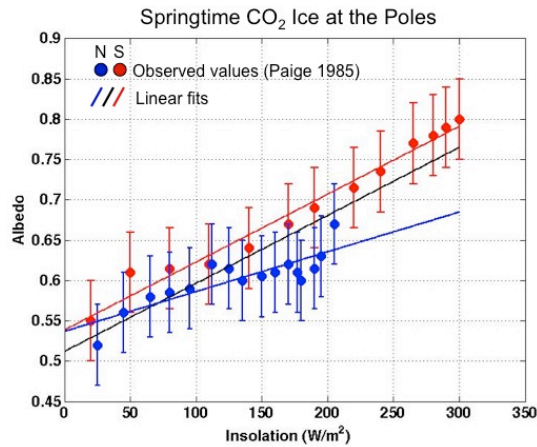


**Figure 7** – Values for the solar albedo of seasonal CO<sub>2</sub> ice deposits on the residual caps obtained from Viking IRTM observations of apparent albedo using a model to remove the atmospheric contribution [5], plotted as a function of the incident solar flux at the surface. Blue circles correspond to northern hemisphere and red to southern. Colored lines are linear fits to the measured values in each hemisphere (used for simulation shown in Fig. 8), and the black line is a fit to all values.

here, perhaps during a favorable high obliquity period in the past 1 Myr, then it would nearly double the global mean surface pressure which could have significant climatic effects related to aeolian transport and liquid water stability among others [1]. In order to explore its potential effects on past atmospheric collapse and subsurface warming, we performed some model simulations with a doubled CO<sub>2</sub> inventory (400 kg/m<sup>2</sup> global). An example of our results is shown in **Fig. 8**, for a case in which we also used an insolation- and hemisphere-dependent CO<sub>2</sub> frost albedo (linear fits in Fig. 7). Although the albedo effect resulted in thick perennial CO<sub>2</sub> caps during some high obliquity periods, there were several times when the atmospheric pressure reached 1000-1200 Pa followed by a rapid drop to <100 Pa, which could produce a greater degree of subsurface warming than our previous estimates. Finally, we note that this model also produces perennial CO<sub>2</sub> ice deposits at the south pole which are comparable in thickness to the buried deposit recently detected there [1].

**Acknowledgements:** This work was supported by NASA Exobiology Program grant NNX08AP63G.

**References:** [1] Phillips, R.J. *et al.* (2011), *Science* v332 pp. 838-841. [2] Presley, M.A. and P.R. Christensen, *J. Geophys. Res.*, 102, 6551–6566. [3] Wood, S.E. and S.D. Griffiths (2009) 40<sup>th</sup> LPSC, Abstract #2490. [4] Wood, S. E. and D. A. Paige (1992) *Icarus* 99, 1-14. [5] Paige, D. A. and A. P. Ingersoll (1985) *Science* 228, 1160-1168. [6] Haberle, R. M. *et al.* (2007). [7] Hansen, G.B. (1999). [8] Laskar, J. *et al.* (2004) *Icarus*, 170, 343-364. [9] Armstrong, J. C. *et al*

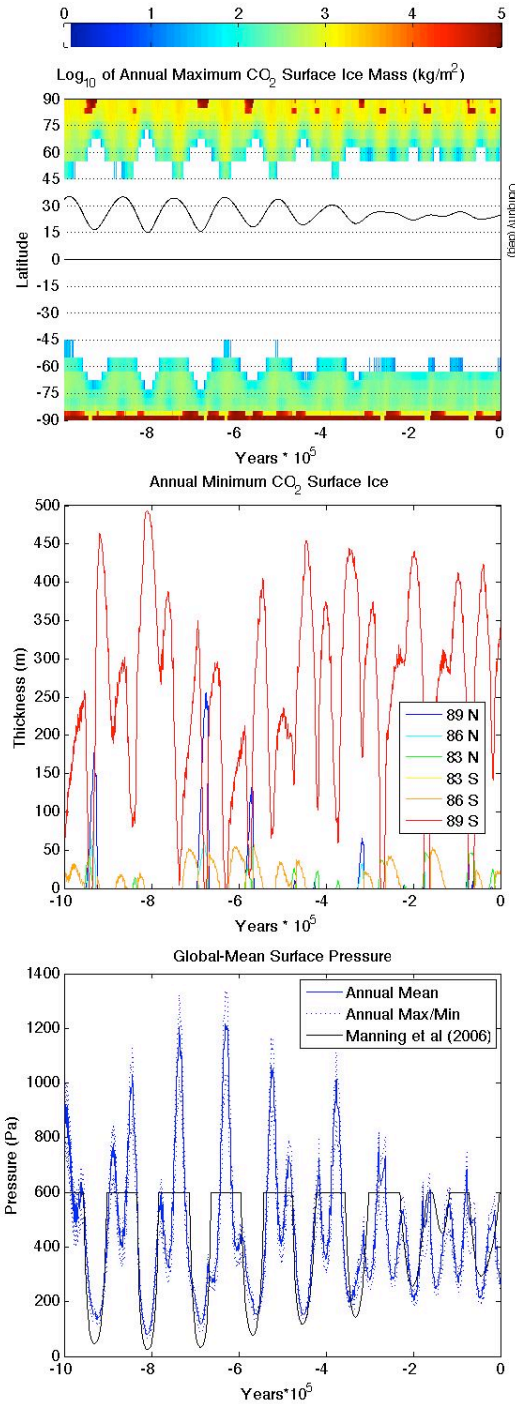


**Figure 8** – (A,B) Same as Fig. 6, but for case with doubled CO<sub>2</sub> inventory and insolation-dependent  $A_f$ . (C) Corresponding model-calculated variations in annual mean surface pressure (blue solid line) as well as the range of seasonal variations (dotted blue lines).

(2004) *Icarus* 171, 255-271. [10] Manning, C. V. *et al.* (2006) *Icarus*, 180, 38-59. [11] Byrne, S. (2009), *Annu. Rev. Earth Planet. Sci.* 37:8.1-8.26. [12] Guo, X. *et al* (2010), *J. Geophys. Res.* 115, E04005.